

Electron-spin double resonance by longitudinal detection.

II. Signal dependence on relaxation times

M. Martinelli, L. Pardi, C. Pinzino, and S. Santucci

Istituto di Fisica dell'Università, Pisa, Italy

and Gruppo Nazionale di Struttura della Materia del Consiglio Nazionale delle Ricerche, Pisa, Italy

(Received 5 November 1975)

The line shape of the longitudinally detected electron-spin-resonance (LODESR) signal is studied as a function of the relaxation times of the considered spin system. Assuming low saturation as an approximation, analytical expressions of intensity and linewidth are obtained for the signals due to some main harmonics. These results are compared with experiments performed on different spin systems in solids. Direct measurements of microwave field strength in the resonant cavity have been obtained by a new technique using the field-induced shift of the resonance frequency of a spin sample. Comparison of LODESR method with some other double-resonance effects is discussed. Finally, it is shown with experiments that the LODESR method provides in a simple way an immediate measure of variations of longitudinal relaxation times.

I. INTRODUCTION

In a previous paper¹ (hereafter referred as I) we considered an electron-spin system irradiated with two transversal waves at angular frequencies ω_r and ω_s , both near to the resonance frequency ω_0 of the system; in I we showed that the longitudinal component of the magnetization oscillates with an angular frequency $|\omega_r - \omega_s|$ and its multiples. Then, longitudinal detection of electron-spin resonance (LODESR)² could be used to resolve superimposed paramagnetic spectra in a mixture of different spin systems.

In fact, the response of spin species having slower longitudinal relaxation is enhanced over the spin systems with fast relaxation times. Note that such a behavior is just the opposite of what occurs in usual electron paramagnetic resonance when saturation is reached.

However, detailed implications of the theory of I were only numerically developed. In this paper we present new analytical derivations concerning some phenomena of actual experimental interest.

In Sec. II we consider the theory regarding the LODESR signal leading to analytical formulas related to such topics as linewidth, saturation, intensities of harmonics, shape, and dependence on relaxation times.

In particular we offer further evidence about the main advantage of the LODESR method, that is, the linear dependence on longitudinal relaxation time T_1 of the first harmonics of the detected signal. From a practical point of view, this allows a straightforward and direct measurement of the variations of T_1 in contrast to the usual saturation method.

In Sec. III we present some new experimental techniques to improve the apparatus used in

LODESR signal detection. In particular we succeeded in measuring the e.m. field intensities directly inside the resonant cavity. Information about the field amplitude is derived from the shift of the ESR signal detected with one e.m. wave, while another wave irradiates the sample with a varying level of power. Such a procedure turns out not to depend on relaxation times.

Section IV contains experimental results confirming theory, and a thorough discussion.

II. THEORETICAL SECTION

The response of a spin- $\frac{1}{2}$ system at paramagnetic resonance transversally irradiated by two e.m. waves is thoroughly considered in I, to which we refer for more details. In our treatment we use second quantization to describe e.m. fields; the operators acting on the total system (fields plus spins) are represented on the basis

$$|m, n_r, n_s\rangle, \quad (1)$$

where m is the spin z -component quantum number and n_r, n_s are the photon occupation number of the two waves.

The total Hamiltonian can be written

$$\mathcal{H} = \mathcal{H}_S + \mathcal{H}_R + \mathcal{H}_I.$$

Assuming $\hbar = 1$, the Hamiltonians of the isolated spin system and of the radiations are

$$\mathcal{H}_S = \omega_0 S_z$$

and

$$\mathcal{H}_R = \mathcal{H}_R^{(r)} + \mathcal{H}_R^{(s)} = (\omega_r a_r^\dagger a_r + \omega_s a_s^\dagger a_s),$$

respectively, while the interaction Hamiltonian is given by

$$\begin{aligned} \mathcal{H}_I = \mathcal{H}_I^{(r)} + \mathcal{H}_I^{(s)} = g\mu_B(\omega_r/2V)^{1/2}(a_r^\dagger + a_r)S_x \\ + g\mu_B(\omega_s/2V)^{1/2}(a_s^\dagger + a_s)S_x. \end{aligned}$$

In the above equations, $\omega_0 = g\mu_B H_0$; a_s, a_r and a_s^\dagger, a_r^\dagger are the annihilation and the creation operators for the two waves, respectively, V is the volume in which the e.m. waves are contained and μ_B is the Bohr magneton.

In order to obtain the response of the spin system we need only consider a nearly degenerate manifold of eigenstates of the Hamiltonian $\mathcal{H}_S + \mathcal{H}_R$.³ The states (1) which we consider here can be ordered in the succession

$$\begin{aligned} \dots |+\frac{1}{2}, n_r+1, n_s-1\rangle, |-\frac{1}{2}, n_r+1, n_s\rangle, \\ |+\frac{1}{2}, n_r, n_s\rangle, |-\frac{1}{2}, n_r, n_s+1\rangle, \\ |+\frac{1}{2}, n_r-1, n_s+1\rangle, |-\frac{1}{2}, n_r-1, n_s+2\rangle, \dots \end{aligned} \quad (2)$$

labeling them with $\dots -2, -1, 0, 1, 2, 3, \dots$. The label 0 corresponds to the state $|+\frac{1}{2}, n_r, n_s\rangle$.

Let us write the density operator for the total interacting spin-radiation system as $\rho = \rho_0 + D$,³ where D contains the full effect of the relaxation mechanism, and ρ_0 is the density operator at thermodynamic equilibrium. It is shown elsewhere^{3,4} that the operator D obeys the relation

$$\frac{i}{\tau} D = [\mathcal{H}_I, D] - \frac{\beta[\mathcal{H}_R, \mathcal{H}_I]}{\text{Tr}[\exp - \beta(\mathcal{H}_S + \mathcal{H}_I)]}, \quad (3)$$

where we introduce τ as the relaxation superoperator; $\beta = 1/kT$ is the usual Boltzmann factor.

In order to estimate the k th harmonic of the longitudinal component of the magnetization M_z with respect to $(\omega_r - \omega_s)$ we have just to calculate the statistical average⁴

$$\langle g\mu_B S_z a_r^\dagger a_s^\dagger \alpha_r^k \alpha_s^k \rangle / \alpha_r^{*k} \alpha_s^k = g\mu_B \text{Tr}(D S_z a_r^\dagger a_s^\dagger \alpha_r^k \alpha_s^k) / \alpha_r^{*k} \alpha_s^k. \quad (4)$$

α_r and α_s are the expectation values of a_r and a_s on their coherent states.

Equation (3), if represented on the basis system (1) labeled as in (2), becomes a linear algebraic system for the matrix elements $D_{i,j}$.

We note that due to the high number of photons n_r and n_s the states $|m, n_r, n_s\rangle$ and $|m, n_r+1, n_s-1\rangle$ are physically equivalent. This implies the recurrence rule

$$D_{i,j} = D_{i+2k, j+2k}. \quad (5)$$

Thus, from (4) and (5) we get

$$\frac{1}{2} g\mu_B N(D_{0,2} - D_{1,3}) + \text{c. c.}$$

for the first harmonics (i.e., $k=1$) in $(\omega_r - \omega_s)$,

$$\frac{1}{2} g\mu_B N(D_{0,4} - D_{1,5}) + \text{c. c.}$$

for the second one, and for the n th harmonics,

$$\frac{1}{2} g\mu_B N(D_{0,2n} - D_{1,2n+1}) + \text{c. c.}; \quad (6)$$

N is the number of spins in the unit volume.

We specify the $1/\tau$ superoperator assuming $[(i/\tau)D]_{i,j} = (i/T_{i,j})D_{i,j}$, with $T_{i,j} = T_1$, if the matrix elements $D_{i,j}$ is taken between two states corresponding to the same spin eigenvalues ($i-j$ is an even number) and $T_{i,j} = T_2$ otherwise ($i-j$ is an odd number).

In order to solve the linear algebraic system for $D_{i,j}$, we point out that $|j-i|$ is the number of photons involved in the transition between the state i and the state j , as is apparent by direct inspection to the succession (2).

We then neglect the elements $D_{i,j}$ with $|i-j|$ larger than the greatest number of photons detectable in our actual experiment.

Using this approximation and (5), we obtain

$$D_{0,2n} = -D_{1,2n+1}.$$

Moreover, we obtain from (3) the basic equations for the matrix elements of the operator D :

$$\begin{aligned} (i/T_1)D_{0,2n} = \lambda_r(D_{1,2n+2} - D_{0,2n-1}) \\ + \lambda_s(D_{1,2n} - D_{0,2n+1}) - n\Delta_2 D_{0,2n}, \end{aligned} \quad (7)$$

$$\begin{aligned} (i/T_2)D_{0,2n-1} = -2\lambda_r D_{0,2n} - 2\lambda_s D_{0,2n-2} \\ - [\Delta_1 + (n-1)\Delta_2]D_{0,2n-1} + \lambda_s \omega_s A, \end{aligned} \quad (8)$$

$$\begin{aligned} (i/T_2)D_{1,2} = 2\lambda_r D_{0,2n-2} + 2\lambda_s D_{0,2n} \\ + (\Delta_1 - n\Delta_2)D_{1,2n} - \lambda_r \omega_r A. \end{aligned} \quad (8')$$

In the above equations λ_r and λ_s are the matrix elements of \mathcal{H}_I for the r and s wave, respectively; $\Delta_1 = \omega_s - \omega_0$, $\Delta_2 = \omega_s - \omega_r$, and A is zero where $n \neq 1$, and otherwise is β/p , where p the number of the states [Eq. (1)] which are considered.

We can estimate λ_r and λ_s , through a classical representation of the fields $H_x^{(\alpha)} = 2H_1^{(\alpha)} \cos \omega_\alpha t$ ($\alpha = r, s$), to give (for a spin- $\frac{1}{2}$ system)

$$\lambda_r = \frac{1}{2} g\mu_B H_1^{(r)} \quad \text{and} \quad \lambda_s = \frac{1}{2} g\mu_B H_1^{(s)}.$$

Note that the matrix elements $D_{0,2n}$ taken between states with the same spin z -component quantum number contribute to the longitudinal \vec{M} component (6), while the matrix elements $D_{0,2n+1}$ and $D_{1,2n}$ taken between states with $\Delta m = \pm 1$ contribute to the transverse component of \vec{M} . By direct inspection of Eq. (7) it is clearly seen how relaxation processes couple the transverse and longitudinal components of \vec{M} .

Assuming $\lambda_s = \lambda_r = \lambda$, the lowest-order approximation gives $D_{0,1}$ and $D_{1,2}$ linear in λ , $D_{0,0}$, $D_{1,1}$, $D_{0,2}$, and $D_{1,3}$ quadratic in λ .

In general, in the lowest-order approximation, the terms $D_{0,2n}$ and $D_{1,2n+1}$ are proportional to λ^{2n} ,

while the terms $D_{0,2n+1}$ and $D_{1,2n+2}$ go as λ^{2n+1} .

The matrix element $D_{0,2n}$ involves a $2n$ -photon process and directly contributes to the n th harmonics in Δ_2 of the longitudinal magnetization.

If, on some physical basis, one chooses a number $2K$ such that processes involving more than $2K$ photons can be neglected, it is possible to obtain separate recurrence rules for the matrix elements of D contributing to longitudinal and transversal \vec{M} components.

Let us now look for solutions of Eqs. (7), (8), and (8'). We limit ourselves to cases which can be actually realized in laboratory practice, that is we assume that the following conditions hold:

$$\lambda_r = \lambda_s = \lambda, \quad |K\Delta_2| \ll 1/T_1, \quad |K\Delta_2| \ll 1/T_2. \quad (9)$$

To simplify notations, let us define $D_n = D_{0,2n}$ and $D_{-n} = D_{0,2n}^*$. By substitution of Eqs. (8) and (8') in (7), a bit of algebra yields

$$D_n = -S(L+S)^{-1}(D_{n-1} + D_{n+1} + C_n) \quad (10)$$

with $S = 4\lambda^2 T_1 T_2$, $L = 1 + (\omega_0 - \omega')^2 T_2^2 + S$, $\omega' = \frac{1}{2}(\omega_r + \omega_s)$, and $C_n = 0$ if $|n| \geq 2$, $2C_1 = 2C_{-1} = C_0 = -\omega' A$.

We now compute (10) for $n=K$, that is, we neglect processes involving more than $2K$ photons; by consistently omitting in Eqs. (7), (8), and (8') terms going as λ^{2K+1} and successive powers, we find, for the last considered terms,

$$\begin{aligned} D_{K-1} &= -S(L+S)^{-1}(D_{K-2} + C_{K-1}), \\ D_K &= -S(L-S)^{-1}(D_{K-1} + C_K). \end{aligned} \quad (11)$$

Finally, Eq. (11) and repeated use of Eq. (10) give the term contributing to the first-harmonics component of M_z for $K > 1$

$$D_1 = -S(L+S)^{-1}(D_0 + f(K)D_1 + C_1). \quad (12)$$

The function $f(K)$ appearing in (12) is real and depends on the value of K ; analytical expressions for $f(K)$ are easily obtained giving, for instance,

$$f(2) = 0, \quad f(3) = -S/(L+S).$$

Note that because of approximations (9) all the terms D_n obtained through Eqs. (10) and (12) turn out to be real.

Now we consider in more detail the terms contributing to the first- and the second-harmonics components of M_z . An approximation with six photons ($K=3$) is usually sufficient; thus from (10) and (12) one gets

$$D_1 = -SC_1(L-S)/[(L+S)^2 - 3S^2], \quad (13)$$

$$D_2 = S^2 C_1 (L-S)/[(L+S)^3 - 3S^2(L+S)]. \quad (13')$$

In particular, for low values of the saturation factor ($S \ll 1$), Eq. (13') becomes

$$D_1 = -SC_1[1 + (\omega_0 - \omega')^2 T_2^2]^{-1}. \quad (13'')$$

Equation (13'') shows how the LODESR signal is proportional to the product $T_1 \circ T_2$. In the same approximation, one has for the higher-order harmonics

$$D_n = (-S)^n C_1 (L-S)^{-n}. \quad (14)$$

Thus, if $S \ll 1$, only one maximum can appear in the line shape of every harmonics. Moreover, from Eq. (14) it can be seen that the higher n , the narrower is the line shape. In particular the value of D_n reaches half of its maximum value when

$$\omega_0 - \omega' = \pm(2^{1/n} - 1)^{1/2}/T_2. \quad (15)$$

The dependence of D_1 on the static magnetic field can also be inferred from Eq. (13), and it is easily seen that, when $S \leq 1$, only one maximum appears, which occurs at $\omega_0 = \omega'$. Taking $\omega_0 = \omega'$, D_1 increases with S as $D_1 = SC_1(1 + 4S + S^2)^{-1}$, and reaches its maximum when $S=1$. Then, for greater S , D_1 decreases and in its line shape versus ω_0 two peaks appear for

$$\omega_0 = \omega' \pm (S-1)^{1/2}/T_2. \quad (16)$$

Note that for ω_0 given by Eq. (16), $D_1 = \frac{1}{6}C_0$ whatever S is. In the same way, from (13) the full width at half amplitude for the signal due to D_1 is given by

$$\Delta_{1/2} = (2/T_2) \{S(S+2) + [(S+1)^4 - S^2]^{1/2}\}^{1/2}. \quad (17)$$

III. EXPERIMENT

We refer to I for the description and details of our experimental apparatus. Here, we discuss only new features and improvements that have been introduced in performing the measurements presented in this paper. First, the range of frequency lock between the two klystrons has been increased to the whole bandwidth of the resonant cavity; second, the harmonic products in the beat frequency have been considerably reduced (70 dB instead of 20 dB below carrier for the second harmonics). Finally, we have set up a new technique to measure the amplitude of microwave magnetic fields inside the resonant cavity. This is particularly important when measuring the relaxation times by the saturation method, which is noticeably affected by inaccurate measurement of the field. In fact, the field amplitudes are usually derived once the impinging microwave power and the merit factor Q of the resonant cavity are known. However the presence of dielectric or conducting materials in the cavity can remarkably modify the distribution of the fields. For instance, inserting a quartz Dewar for low temperatures in

a standard ESR cavity increases the field amplitude on the sample by about two times.⁵

To overcome the above difficulty, we succeeded in determining the amplitude of the microwave field through a direct measurement of the radiation-induced shift of one ESR line. To do this, we detect the transverse paramagnetic resonance of the sample placed in the cavity at the frequency ω' , at the same time the sample was irradiated with another wave with frequency $\bar{\omega}$. These two microwave fields at frequency ω' and $\bar{\omega}$ were parallel to each other and both frequencies were kept fixed; only the power of the wave with frequency ω' was varied. In such condition the magnetic field of resonance is shifted by an amount which is given by⁶

$$\omega_0 - \omega' = (\bar{\omega} - \omega') - [(\bar{\omega} - \omega')^2 - 4\bar{\lambda}^2]^{1/2}$$

with

$$\bar{\lambda} = g\mu_B \bar{H}_1 / 2\hbar.$$

In Fig. 1 we show the amplitude of microwave magnetic field $2\bar{H}_1$ versus the shift of paramagnetic resonance $\delta = \hbar(\omega_0 - \omega')/g\mu_B$. The sample used in the experience of Fig. 1 was a radical system obtained by electrolytic deposition of oxypyrrrol; its

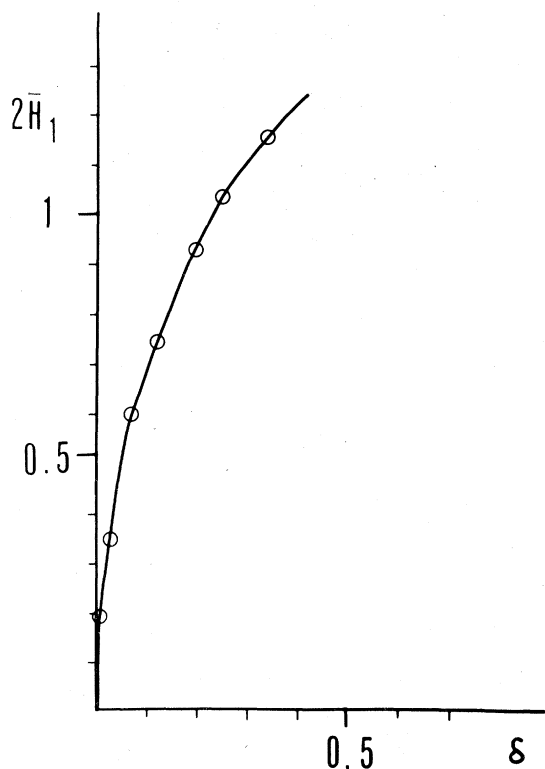


FIG. 1. Amplitude of microwave magnetic field $2\bar{H}_1$ vs $\delta = \hbar(\omega_0 - \omega')/g\mu_B$ as measured inside the cavity. The quantities δ and $2\bar{H}_1$ are in gauss.

relaxation time is $T_2 = 3.1 \times 10^{-7}$ sec. The wave of frequency $\bar{\omega}$ was produced by a klystron VA197W, frequency locked to the resonance frequency of the cavity. The other wave was produced by a klystron X13 and its frequency was kept at a difference of 1.86 MHz from the frequency $\bar{\omega}$.

IV. RESULTS AND DISCUSSION

In this section we discuss some experiments by which we applied and tested the theoretical results reported in Sec. II.

In Fig. 2, the LODESR signal due to the first [Fig. 2(a)] and the second [Fig. 2(b)] harmonics of the oscillations of M_z are shown. The difference between the frequencies of the two impinging waves is $\Delta_2/2\pi = 80$ KHz. In the case of Fig. 2 the spin system was supplied by Mn^{++} ions in MgO crystal. The static magnetic field H_0 was directed along the [111] crystal axis.

Since Mn^{++} has $S = \frac{5}{2}$ and $I = \frac{5}{2}$, 30 resonance lines are expected.⁷ In Fig. 2 only the part of the spectrum corresponding to $m = \frac{5}{2}$ is reported. The central line corresponds to the transition $M_s = -\frac{1}{2} \rightarrow M_s = +\frac{1}{2}$, the intermediate lines to the transitions $M_s = \mp\frac{3}{2} \rightarrow M_s = \mp\frac{3}{2}$ and the other lines to the $M_s = \mp\frac{3}{2} \rightarrow M_s = \mp\frac{1}{2}$.

The different widths of the resonance lines in Fig. 2 are due to internal stresses of the crystal. The direction [111] of the static field H_0 , has been chosen in order to minimize these effects.⁸

As it is apparent from Fig. 2, the signal is obtained in nonderivative shape; moreover it shows linear and quadratic dependence on the saturation factor for the first and the second harmonics, respectively.

The reader should have noticed that the theoretical findings of Sec. II hold for a spin- $\frac{1}{2}$ system. If $S \neq \frac{1}{2}$ the matrix elements of the field-spin inter-

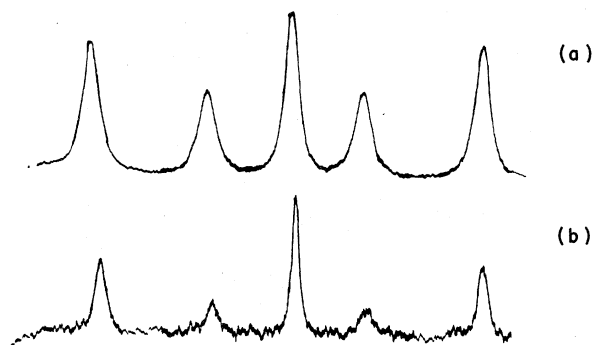


FIG. 2. (a) First- and (b) second-harmonics LODESR signal for Mn^{++} in MgO. The reported curves correspond to $m = \frac{5}{2}$ and to the static field H_0 along the [111] direction.

action Hamiltonian \mathcal{H}_r , between a state with spin quantum number M_S and a state with spin quantum numbers $M_S \pm 1$, $\langle M_S | \mathcal{H}_r | M_S \pm 1 \rangle$, are obtained from the corresponding matrix elements for $S = \frac{1}{2}$, just by multiplying them with the factor $[S(S+1) - M(M \pm 1)]^{1/2}$.

In our case, the theoretical amplitudes of the lines of Fig. 2 are in the ratio 8:5:9:5:8 for the LODESR first harmonics. For the second harmonics, the ratios are the square of the previous ones.

In Fig. 3, using the same sample as before, we show the dependence on the saturation factor S of the linewidth, for the first [Fig. 3(a)] and for the second [Fig. 3(b)] harmonics, corresponding to the transition $M_S = -\frac{1}{2} \rightarrow M_S = +\frac{1}{2}$, $m_r = \frac{5}{2}$. More exactly, in Fig. 3 we plot the quantity R , defined as the ratio of the above linewidths with the unsaturated first-harmonics linewidth. In Fig. 3(a), the solid line represents the theoretical result obtained from Eq. (17). Use of Eq. (15) yields the ratio approximately 0.64 between the linewidth of the second and the first harmonics, for low values of the saturation factor S (look at Fig. 3 for the agreement with experiment). Note that as other authors report,⁹ in the usual transverse detection of transitions involving $2n+1$ photons, the linewidth decreases as $(2n+1)^{-1}$. In contrast, we obtain by LODESR, and deduce using Eq. (15), that the linewidth has a smoother decrease as the number of photons involved increases. The main reason for this result in our case, is that we use two waves both with an angular frequency $\approx \omega_0$. In other methods using transverse detection, just the sum of the energies of the photons involved is

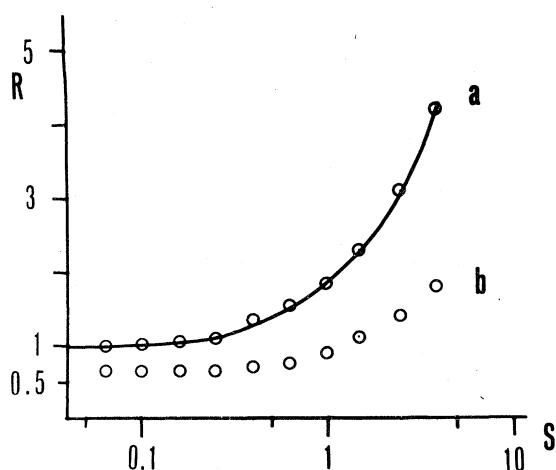


FIG. 3. Linewidth for the (a) first- and (b) second-harmonics LODESR signal versus the saturation factor S for the transition $M = \frac{1}{2} \rightarrow M' = -\frac{1}{2}$, $m = \frac{5}{2}$ of Mn^{++} in MgO . R is measured in units of unsaturated first-harmonics linewidth.

equal to the energy of the transition considered. In Sec. II we have shown that the signal due to the first harmonics has the characteristic two-peaked shape when the saturation factor $S > 1$.

Similar effects occur in several fields of the spectroscopy. In the Autler-Townes effect,¹⁰ in optical pumping,¹¹ in spin-tickling experiments of nuclear magnetic resonance,¹² or also in microwave-double-resonance spectroscopy¹³ the typical system of interest has three levels $|a\rangle$, $|b\rangle$, and $|c\rangle$. The system is then irradiated by an intense wave of frequency nearly resonant with the transition $|a\rangle \rightarrow |b\rangle$. In turn, detection is made by means of a further wave whose frequency is nearly resonant with the transition $|b\rangle \rightarrow |c\rangle$. Once an edge in the intensity of the first wave is reached, the signal appears with the typical two-peaked shape. The two peaks are symmetric only if the first wave is exactly resonant with the irradiated transition. Note that, in our case, the relative symmetry of the peaks is independent of the distance between the frequencies, and only requires equality of the intensities of the two waves.

The distance between the two peaks of the first harmonic signal is plotted in Fig. 4 as a function of the saturation factor. The solid line represents the theoretical results given by Eq. (16). Experimental points in Fig. 4 were obtained using as spin system a sample of electrolytical radical of oxypryrrol.

The relaxation times of the system are strongly affected by the presence of oxygen in the electrolytic bath and by the current intensity and temperature of the bath. Also in standard conditions we found it very difficult to always obtain samples with the same physical characteristics, and the repeatability of measurements is seldom achieved.

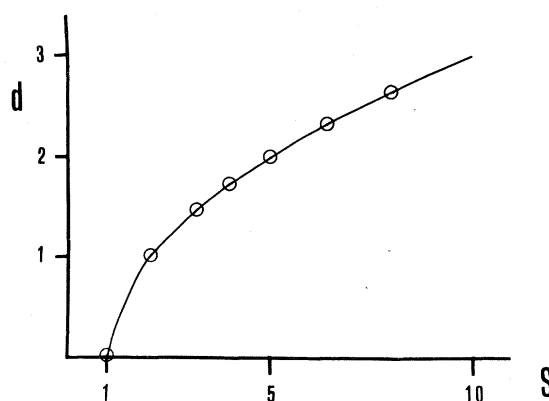


FIG. 4. Distance between the two peaks measured in gauss, for increasing values of saturation factor. The solid line represents the theoretical results given by Eq. (12). The experimental points are obtained with a radical of oxypryrrol.

The sample of Fig. 4, had $T_1 = 1.23 \times 10^{-6}$ sec and $T_2 = 3.1 \times 10^{-7}$ sec at room temperature.

We wish now to comment about experiments of second-harmonics generation by Boscaino *et al.*¹⁴ The two peaks they discuss are shifted apart by the same amount as required by our Eq. (16). Such an agreement between our result and the one by Boscaino *et al.* is obtained if we take into account processes up to six photons, as are included in Eq. (16). On the other hand, the theoretical results of Ref. 14 are obtained in the two-photon approximation. If we too make the same approximation, our theoretical line has then only one peak. By going to a four-photon approximation we obtain a line shape with two peaks, but their distance is now given by $d = 2T_2^{-1}[S(2)^{1/2} - 1]^{1/2}$, which is greater than the one deduced from Eq. (16).

The LODESR phenomenon, as discussed here and elsewhere¹ shares many characteristics with second-harmonic generation, which however is unfavored by its low probability of occurring. Harmonic generation, in fact, involves only processes of second-order or higher in the spin-field interaction, while the effect we study here is due to two separate first-order processes. Due to this, the amplitude probability of harmonics generation is reduced by a factor of order $(\hbar\omega)^{-1}|\langle \mathcal{H}_I \rangle|^2$ or greater, thus requiring experimental apparatus at very low temperatures, with very high powers, and with samples containing a high density of spins. Using harmonic generation in standard paramagnetic resonance studies turns out to be very difficult.

How powerful our method is in measuring the variation of the longitudinal relaxation time can be realized from Fig. 5. Here, in the lower part, we report the usual ESR signal received from the system $\text{Mn}(\text{NO}_3)_2$ in 0.05-mole% H_2O solution at different temperatures.¹⁵ In the upper part of the figure the first harmonics of the LODESR signal is reported for the same sample at the same temperatures. It is apparent that in the ESR signal,

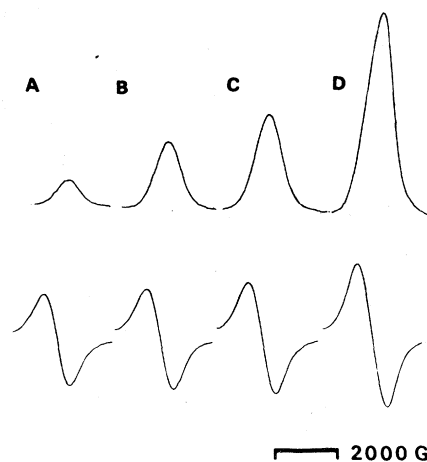


FIG. 5. ESR (down) and LODESR (upper) signals of $\text{Mn}(\text{NO}_3)_2$ in 0.05-mole % H_2O solution at different temperatures: 182 °K (A), 163 °K (B), 143 °K (C), 104 °K (D).

the variations are only due to the factor kT . On the contrary, the LODESR signal, far from saturation, is proportional to the product $T_1 T_2$; thus the variation of T_1 can be directly inferred from variations of the detected signal. From LODESR measurements in the high-temperature range, dependence of T_1 on T^{-2} is revealed. This can be explained through two-photon Raman processes.¹⁶

In conclusion, we note that above experimental technique is remarkably simpler and cheaper than pulse-saturation method, as a procedure to obtain variations of relaxation times. In fact, the usual pulse technique requires high power and very speedy electronic apparatus, and does not apply very well to the case of high temperature. On the contrary, the measurement method presented here works quite well over a large temperature range.

ACKNOWLEDGMENT

The authors are very indebted to A. Pistoiesi for help in setting up the electronics experimental apparatus.

¹F. Chiarini, M. Martinelli, L. Pardi, and S. Santucci, *Phys. Rev. B* **12**, 847 (1975).

²M. Martinelli, L. Pardi, C. Pinzino, and S. Santucci, *Solid State Commun.* **17**, 211 (1975).

³A. Di Giacomo and S. Santucci, *Nuovo Cimento B* **63**, 407 (1968).

⁴P. Bucci, M. Martinelli, and S. Santucci, *J. Chem. Phys.* **53**, 4524 (1970).

⁵C. P. Poole, Jr., *Electron Spin Resonance* (Interscience, New York, 1967).

⁶F. Chiarini, M. Martinelli, P. A. Rolla, and S. Santucci, *Nuovo Cimento Lett.* **5**, 197 (1972).

⁷W. Low, *Phys. Rev.* **101**, 1827 (1956).

⁸E. Rosenwasser Feher, *Phys. Rev. A* **136**, 145 (1964).

⁹S. Yatsiv, *Phys. Rev.* **113**, 1522 (1959); **113**, 1538

(1959). *J. Winter*, *Ann. Phys.* **19**, 746 (1959).

¹⁰S. H. Autler and C. H. Townes, *Phys. Rev.* **100**, 753 (1955).

¹¹J. Brossel, *Rendiconti della Scuola di Varenna XVII Corso* (Academic, New York, 1962).

¹²A. Abragam, *The Principles of the Nuclear Magnetism* (Clarendon, Oxford, 1960).

¹³T. Oka and T. Shimizu, *Phys. Rev. A* **2**, 587 (1970).

¹⁴R. Boscaino, I. Ciccarello, C. Cusumano, and M. W. P. Strandberg, *Phys. Rev. B* **3**, 2675 (1971).

¹⁵F. M. Gumerov, B. M. Kozyrev, and G. P. Vishnevskaja, *Mol. Phys.* **29**, 937 (1975).

¹⁶A. Abragam and B. Bleaney, *Electron Paramagnetic Resonance of Transition Ions* (Clarendon, Oxford, 1970).